Exciton localization, photoluminescence spectra, and interface roughness in thin quantum wells

U. Jahn, S. H. Kwok, M. Ramsteiner, R. Hey, and H. T. Grahn*
Paul-Drude-Institut für Festkörperelektronik Berlin, Hausvogteiplatz 5-7, D-10117 Berlin, Germany

E. Runge
Max-Planck-AG ''Halbleitertheorie,'' Hausvogteiplatz 5-7, D-10117 Berlin, Germany
(Received 20 February 1996)

The combination of conventional photoluminescence (PL), PL-excitation (PLE), and micro-PL spectroscopies is used to study the influence of interface roughness on luminescence properties of thin $GaAs/Al_{0.3}Ga_{0.7}As$ single quantum wells (QWs). The QWs were prepared under different growth conditions, resulting in different interface roughness. We discuss the splitting of PL spectra into two (or more) main lines, the pronounced fine structure of the micro-PL spectra and the low-energy shift of the PL lines with respect to the PLE spectrum in terms of a phenomenological interface model. For low temperatures exciton localization due to interface fluctuations with different length scales determines most of the luminescence features. One consequence is a strong suppression of the PLE signal on the low-energy side of the spectra. Therefore in this case the PLE spectrum cannot be used as a measure for the absorption strength or as an indicator for impurity bound excitons. [S0163-1829(96)03828-3]

I. INTRODUCTION

Optical and electronic properties of semiconductor heterostructures grown by molecular-beam epitaxy (MBE) or metal-organic vapor-phase epitaxy are sensitive to the structure of the interfaces. The interface roughness can involve several components, which differ in the lateral length scale.[1–4] Various methods are available for the investigation of the real structure of *surfaces* on different length scales ranging from the atomic scale to the wafer size (e.g., scanning tunneling and atomic force microscopy, scanning electron microscopy, and optical microscopy). In the case of *interfaces*, however, the situation is more difficult. Applying direct methods such as cross-section transmission electron microscopy (TEM) and scanning tunneling microscopy (STM), heterointerfaces can be imaged with atomic resolution. However, at least for TEM the observation window is limited to several tens of nm. For STM, the sample has to be doped. Consequently, indirect methods such as photoluminescence (PL), cathodoluminescence (CL), or x-ray scattering are often used to study the interface quality of heterostructures such as quantum wells (QWs).[5–8] Many investigations have been devoted to deriving quantitative information about the interface structure by a detailed lineshape analysis of PL spectra or by CL imaging from QWs.[6,9] However, results obtained by direct methods such as TEM and STM on the one side and luminescence methods such as PL and CL on the other side are often controversial concerning the real interface structure and the interpretation of the experimental data from QWs.[1,10] The reason is probably twofold: (i) the PL line shape is determined by lateral exciton transfer between discrete, large interface islands[11] and by exciton localization due to confinement potential fluctuations;[12] (ii) the probing area of the exciton is larger than the respective component of the roughness, which occurs on a nm scale, leading to an averaging process in luminescence experiments and hence to characteristic line shapes.[13] Recently, Brunner *et al.*[14] and Hess *et al.*[15] demonstrated by micro-PL and optical near field PL, respectively, that at least for low temperatures and thin QWs the line shape of PL spectra is determined by the envelope of many very narrow lines due to excitons localized at lateral potential fluctuations.

In this paper we will focus on exciton localization related to interface roughness. Several $GaAs/Al_xGa_{1-x}As$ single quantum wells (SQWs) were grown by MBE in such a way that different interface structures are expected. Excitonic spectra of these SQWs show different, but characteristic, features, which depend on the growth conditions. We combine the results of PL, photoluminescence excitation (PLE), and spatially resolved micro-PL for a unified picture describing the interface structure of these SQWs. All PL spectra and their temperature dependences can be interpreted in terms of exciton localization due to interface roughness with different length scales.

II. EXPERIMENT

Three single QWs (QW1, QW2, QW3) were prepared by MBE. We used (001)GaAs substrates, without intentional crystallographic misorientation (QW2 and QW3) and with a misorientation angle of 2° towards (111)Ga (QW1). The QWs consisted of a 1.4-μm-thick GaAs buffer layer, an 18-nm-thick $Al_{0.3}Ga_{0.7}As$ barrier, a 3.5-nm-thick GaAs well, a 200-nm $Al_{0.3}Ga_{0.7}As$ top barrier, and a 3-nm-thick GaAs cap layer. QW1 and QW2 were fabricated during the same run. The samples were grown at a substrate temperature of 605 °C with a growth rate of 0.34 and 0.49 μm/h for GaAs and $Al_xGa_{1-x}As$, respectively. The As_4-to-Ga beam equivalent pressure ratios amounted to 16 (QW1 and QW2) and 20 (QW3). Under these conditions the surface exhibited a (3×1) to (2×4) surface reconstruction transition for QW1 and QW2 and a (2×4) reconstruction for QW3. The growth was interrupted for 40 s at both QW interfaces to achieve a certain

smoothness. PL and PLE spectra were recorded at 5 K using an Ar^+-laser-pumped tunable Ti:sapphire laser as the excitation source. The diameter of the laser spot amounted to about 100 μm. For the PL measurements we used an excitation energy of about 1.75 eV, i.e., above all ground-state transitions of the QWs. The PL signal was dispersed by a 1-m grating monochromator and recorded by a liquid-nitrogen-cooled charge-coupled device (CCD) array. The PLE signal was dispersed by the same monochromator, but detected by a cooled GaAs photomultiplier using conventional photon counting techniques. Additionally, micro-PL spectra were recorded at 5 K by a DILOR triple-grating Raman spectrometer with a CCD array detector. In this case the PL was excited by an Ar^+ laser at a photon energy of 2.41 eV. The laser beam was focused to a circular spot by a microscope objective with a numerical aperture (NA) equal to 0.55. Using a pinhole aperture at the image plane of the luminescence, the effective probe size was reduced to about 1.5 μm.

III. RESULTS AND DISCUSSION

Our experimental results are summarized in Figs. 1(a)–1(c) showing the PL and micro-PL spectra of the samples QW1–QW3 together with the heavy-hole line of the respective PLE spectra. Most of the published PL spectra resemble one of the spectra in Figs. 1(a)–1(c) or show at least some of their features, even in cases where multiple monolayer (ML) splitting was observed. Five characteristic features derived from the PL/PLE spectra sequence in Fig. 1 are listed below. (For comparison with results of other authors several references are added.)

(i) The PL spectra become more structured from Fig. 1(a) to 1(c). While in Fig. 1(a) line α can be described by a Gaussian line shape, the PL distribution becomes asymmetric in Fig. 1(b), and a second line β becomes visible on the high-energy side. In Fig. 1(c), this second line β is even more pronounced. Moreover, additional satellite peaks α^* and β^* appear in the PL spectrum of QW3.[1,2,6,9,16–20]

(ii) The energy separation between lines α and β is smaller than expected for a variation of the QW thickness by 1 monolayer (ML splitting).[1–3,5,16,21–23]

(iii) The micro-PL reveals that at least each main line α, which corresponds to the low-energy PL line in Figs. 1(b) and 1(c), actually consists of many, very narrow lines (full width at half maximum smaller than 0.1–0.2 meV). Even the spikes of line β in Fig. 1(c) are real spectral features and not just noise, which is confirmed by repetitive measurements. This fine structure disappears for temperatures larger than 50 K.[14,15,24]

(iv) The energy shift between the low-energy PL line α and the PLE spectrum (ΔE_{PLE}) amounts to 5.5 meV for QW1, i.e., for the sample with a misorientation angle of 2°, and about 9 meV for QW2 and QW3 without misorientation.[25]

(v) The PLE signal is strongly suppressed within the spectral range of the low-energy part of the PL spectrum, where the micro-PL spectra show a pronounced fine structure.[5,25]

Following the arguments of Brunner *et al.*,[14] we assign the part of the PL spectra which shows a fine structure in micro-PL experiments to excitons localized at interface defects caused by roughness and composition fluctuations. Since our samples are undoped, and the unintentional doping density is supposed to be less than 10^{14} cm^{-3} in the GaAs layer, i.e., 3.5×10^{7} cm^{-2} for a well thickness of 3.5 nm, we would expect to obtain less than 0.35 spikes per μm^{-2}, when each impurity contributes one line. This is two orders of magnitude less than the number of peaks (30–50) observed in the micro-PL spectra.[26] Moreover, it is not expected that the variation of our growth conditions causes an essential change of the impurity situation in the QWs. Therefore we believe that the low-energy parts of the PL spectra are related to localization of excitons at intrinsic interface defects rather than to impurities. The spectral position of each of the narrow micro-PL lines represents different localization (binding) energies (E_{bx}) of the excitons, which are determined by the size and shape of the interface defects acting as a localization center. In this context, the comparison of micro-PL spectra with conventional PL and PLE spectra can result in information about the contribution of exciton localization connected with interface fluctuations to the shape and position of PL and PLE spectra. One conclusion is that the PL spectra are determined by the envelope of the narrow line distributions and reflect distinct size distributions of interface

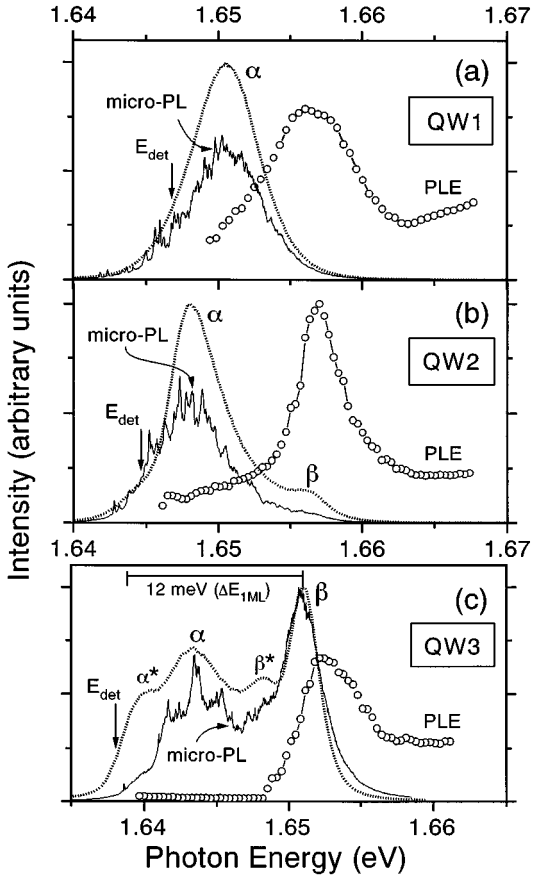

FIG. 1. Photoluminescence (dotted), micro-PL (solid), and PL excitation spectra (open circles) of three GaAs/$Al_{0.3}Ga_{0.7}As$ single QWs at 5 K. For (a) the substrate misorientation angle was 2° towards (111)Ga (QW1), the samples QW2 and QW3 in (b) and (c), respectively, were grown on substrates without crystallographic misorientation. QW1 and QW2 were grown simultaneously with an As_4-to-Ga beam equivalent pressure ratio (BEP) of 16, for QW3 the value of BEP amounted to 20.

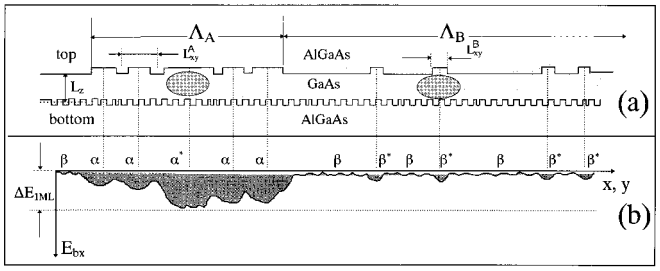

FIG. 2. Schematic sketch of the bottom and top interface of QWs grown on substrates without misorientation (a) and of the resulting lateral variation of the exciton localization energy E_{bx} (b). Λ_A and Λ_B are the lateral sizes of QW regions A and B differing in the mean thickness L_z by about 1 monolayer (ML). L^A_{xy} and L^B_{xy} are the length scales of fluctuations within regions A and B, respectively. Characteristic length scales for the bottom interface are much smaller than those of the top interface. The size of the exciton is sketched by the added ellipses. α, α*, β, and β* indicate QW regions contributing to the corresponding PL lines in Fig. 1(c).

defects. As proposed by Bastard *et al.*[27] back in 1984 within a theoretical model, the Stokes shift between absorption and PL line can be interpreted as mean value of the binding energy E_{bx} of excitons localized at these defects. This energy shift corresponds approximately to the energy shift ΔE_{PLE} between the PL and PLE lines (we will see later that the relation between ΔE_{PLE} and the Stokes shift is not straightforward under conditions of strong exciton localization). The Stokes shift also depends on the details of the carrier relaxation kinetics, which are determined by the carrier temperature, the carrier mobility, and correlation length of the potential fluctuations.[12]

With regard to our experimental results, the decrease of ΔE_{PLE} between the samples without misorientation [Figs. 1(b) and 1(c)] and the one with a 2° misorientation angle [Fig. 1(a)] confirms the model given in Ref. 27 qualitatively, because changing the misorientation angle from 0 to 2° is expected to lead to smaller growth terraces and hence to smaller mean defect sizes. However, the nature of QW interfaces is probably very complex (different lateral shapes of interface islands or holes for given areas are possible, correlation between sizes and shapes of adjacent islands). Therefore the simplified assumption of a semi-Gaussian interface defect with only one parameter for its lateral size in Ref. 27 seems to be not suitable to give a correct quantitative description. It should be noted that for entropy and growth kinetic reasons irregular shapes and fuzzy boundaries are favored whereas energetic arguments favor regular compact shapes and straight boundaries. This is supported by the results of numerical growth simulations (see, e.g., Groβe and Zimmermann[28]). Therefore we do not attempt to describe the PL spectra quantitatively, but discuss our data qualitatively using a phenomenological interface model.

In Fig. 2 this model is illustrated. It contains sketches of the two QW interfaces in (a) and the resulting potential fluctuations experienced by excitons in (b). The nominal QW thickness is L_z. We distinguish between the top and the bottom interface. On the one hand, it is expected that the bottom interface (GaAs on top of $Al_xGa_{1-x}As$) shows microroughness on a nm scale and is usually described as pseudosmooth.[16,28] Such interfaces cause weak, short-range potential fluctuations on a length scale much smaller than the exciton radius ($R_B \approx 10$ nm).[29] On the other hand, we presume a rather flat top interface characterized by a certain distribution of rather large interface defects. In order to get an idea about the nature of this interface, we grew one sample without misorientation under the same conditions as for QW1 and QW2, but stopped the growth after the GaAs layer was completed. Surface images of this sample taken by atomic force microscopy (not shown here) from an area of 1×1 μm^2 show fewer than ten 1-ML steps. Therefore at least this surface, which would be the top interface of the QW, consists of 1-ML-high (deep) growth islands (valleys) with lateral sizes larger than 100 nm. Consequently, it is reasonable to distinguish QW regions A and B with lateral extents Λ_A and Λ_B much larger than R_B, which differ in the mean thickness $\langle L_z \rangle$ by about 1 ML [cf. Fig. 2(a)]. Furthermore, within the narrower QW regions B (completed growth islands of the last of n GaAs monolayers) the probability is large that 1-ML-high *nanoislands* with lateral sizes $L^B_{xy} < R_B$ remain. Within the QW regions A [uncompleted growth islands of the $(n+1)$th GaAs monolayer], however, it is more probable that 1-ML-deep *holes* with distances L^A_{xy} between each other remain. Consequently, the mean thickness $\langle L_z \rangle^A$ ($\langle L_z \rangle^B$), which is the result of averaging over all holes (nanoislands), is determined by the distribution function of L^A_{xy} (L^B_{xy}).

The hole distribution in A and the nanoisland distribution in B cause different potential fluctuations experienced by the center-of-mass motion of the excitons [cf. Fig. 2(b)].[13] Flat parts of regions B correspond to what is usually referred to as free exciton levels. It should, however, be noted that theoretically the center-of-mass wave function is expected to be localized for all exciton eigenstates. Excitons experience shallow potential minima (localization is weak and can be overcome easily by thermal activation) due to the nanoislands within B and deep potential minima (localization is strong) in A. The maximum localization (binding) energy is $\Delta E_{1\ \mathrm{ML}}$, which is the change of the QW confinement energy for a well thickness variation of 1 ML. Within this picture, we will discuss the change of the PL spectra in Fig. 1.

For substrate misorientation angles of 2° (QW1) the sizes of growth terraces are expected to be not larger than about 8 nm, i.e., smaller than $R_B \approx 10$ nm. Therefore the probed excitons cannot distinguish different terraces A and B and the PL spectrum consists of only one main line α [cf. Fig. 1(a)]. The energy shift between α and the PLE line of about 5 meV as well as the well-pronounced fine structure of the micro-PL spectrum indicate that the excitons are localized at potential minima. The two lines α and β appearing in the PL spectra of QW2 and QW3 are due to the existence of large growth terraces A and B as expected for the present growth conditions, when the misorientation angle is nearly 0°. Although the area densities of regions A and B are about the same in QW2 (see below), the PL line α dominates in the case shown in Fig. 1(b), because excitons can be transferred from B to A before radiative recombination can take place. Therefore the Stokes shift seems at first sight to be remarkably increased from QW1 to QW2. Actually, in Figs. 1(b) and 1(c) the PLE band belongs to line β, and the PLE signal of the QW region A is suppressed.

For the interpretation of the high-energy lines β and β^* we focus on sample QW3 because they are well pronounced in that case due to a large area ratio between B and A regions (see below). Its micro-PL spectrum shows a fine structure within almost the whole spectral range. Therefore we argue that even in the high-energy regions B excitons are well localized. However, the narrow lines become weaker and their energy separation smaller with increasing photon energy, and they disappear within the high-energy tail of line β, indicating a decrease of the localization strength from line α to β.

In terms of the model sketched in Fig. 2 we propose the following interpretation. For QW regions B a certain distribution of nanoislands causes an energy shift $\Delta E^B_{\mathrm{PLE}}$ of the PL line β which corresponds to a mean value $\langle L_{xy}\rangle^B$ of the nanoisland size. For QW regions A a certain distribution of holes leads to a fluctuating and on average higher potential as expected without any holes. Therefore its main line α is shifted to higher photon energies compared to the expected spectral position for exactly 1 ML thicker QW regions. This high-energy shift amounts to $\Delta E_{1\ \mathrm{ML}}-\Delta E^A_{\mathrm{PLE}}$, which depends on the mean density and size of the holes. The shift of α as well as β leads to a ML splitting ΔE_{PL} of the PL peaks, which is actually smaller than $\Delta E_{1\ \mathrm{ML}}$. In the case of QW2 and QW3, ΔE_{PL} amounts to 7.8 meV compared to $\Delta E_{1\ \mathrm{ML}}=12$ meV. In this sense $\Delta E^B_{\mathrm{PLE}}$ and $\Delta E_{1\ \mathrm{ML}}-\Delta E^A_{\mathrm{PLE}}$ are a measure for the average size of the nanoislands on terraces B and the average distance of holes within terraces A, respectively. Besides these growth-induced asymmetries, differences in the relaxation and optical matrix elements of A and B regions might also contribute to ML shifts smaller than $\Delta E_{1\ \mathrm{ML}}$.

The sketched model is suitable to explain the shape of the PL spectrum in Fig. 1(c) in detail. The appearance of satellite lines in ML split PL spectra of QWs as in the case of QW3 (α^*/α, β^*/β) is often interpreted by the coexistence of free excitons and impurity bound excitons.[9,18,30] We interpret this doublet shape of the PL spectrum in terms of the interface structure of the QW as assumed earlier by Fujiwara, Cingolani, and Ploog.[19] Two arguments led us to this conclusion: (i) the micro-PL spectrum shows a similar fine structure in the spectral range of line β^* as in the one of line α, which we cannot explain by impurities, (ii) the intensity of line β^* does not saturate, when the excitation intensity is increased by four orders of magnitude. This can be derived from the dependence of the intensity ratio of lines β^* and β (I_{β^*}/I_β) on the excitation density in Fig. 3. Instead of a decrease of I_{β^*}/I_β, we find a weak increase within the displayed excitation power range. Therefore we assign β^* to excitons localized at nanoislands of terraces B and the PL line β to excitons, which recombine within defect-free regions of terraces B. The shape of β, its Stokes shift (about 1 meV), and the appearance of spikes in the micro-PL spectrum are probably due to the pseudosmooth bottom interface and/or composition fluctuation in the barrier layers. The line α is assigned to excitons localized at holes of QW regions A. Remarkably, the energy separation of lines α^* and β amounts to almost exactly the value of $\Delta E_{1\ \mathrm{ML}}$. Moreover, the micro-PL spectrum shows no or only very weak fine structure in the spectral range of α^*. The obvious interpretation is that α^* corresponds to almost flat A regions with n MLs and β corresponds to almost flat B regions with $(n+1)$ MLs.

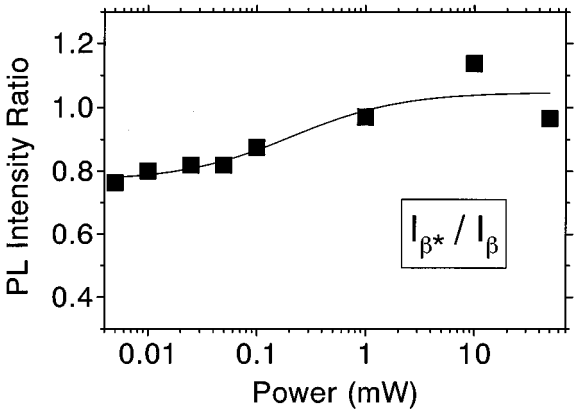

FIG. 3. Ratio of the integrated intensities of the PL lines β and β^* in dependence on the excitation intensity. The values are obtained from fits to the data points assuming Gaussian shaped lines. The solid line is a guide for the eye. The diameter of the laser spot was about 100 μm.

We do not interpret our micro-PL spectra in terms of a QW-dot model as was recently done by Gammon, Snow, and Katzer[24] because the nature of the QW interfaces is too complex to assume sharp potential jumps and simplified lateral shapes for nanoislands or holes. The effective potential localizing excitons is rather smooth.[12,13,29] We calculated center-of-mass wave functions for smooth random potentials. In the low-energy part of the optical spectrum the wave functions are well separated from each other and centered in individual deep potential minima. In the intermediate- and high-energy regions some wave functions are extended over larger regions and appear fractal-like. They can be considered as combinations of excited states in different potential minima. Thus shape and size of potential minima cannot easily be derived from micro-PL or near-field PL spectra.

In Ref. 31 Gurioli *et al.* describe the exciton distribution in a thermalization model even for thin QWs and low temperatures. They argue that the low-temperature theory of Yang *et al.*[32] should not be applied because the carrier temperature (T_c) was found to be considerably higher than the lattice temperature. The validity of respective models depends strongly on the actual experimental conditions. For values of the Stokes shift on the order of or smaller than kT_c,[31] we would expect that thermalization is dominantly effective and determines the PL properties. For growth conditions, however, leading to rather large interface islands, i.e., larger Stokes shifts, as it occurs in our samples prepared by growth-interrupted MBE, exciton trapping determines the shape and temperature dependence of the PL spectra.

We will now discuss the strong suppression of the PLE signal within the spectral ranges, where the micro-PL spectrum shows a pronounced fine structure. In order to estimate the actual density of states in these spectral windows and therefore the expected absorption strength, we used the temperature dependence of the PL intensity ratios between the PL lines α and β in Figs. 1(b) and 1(c). At low temperatures excitons move from terraces B to terraces A [larger average value of $\langle L_z\rangle$ and therefore a smaller exciton confinement

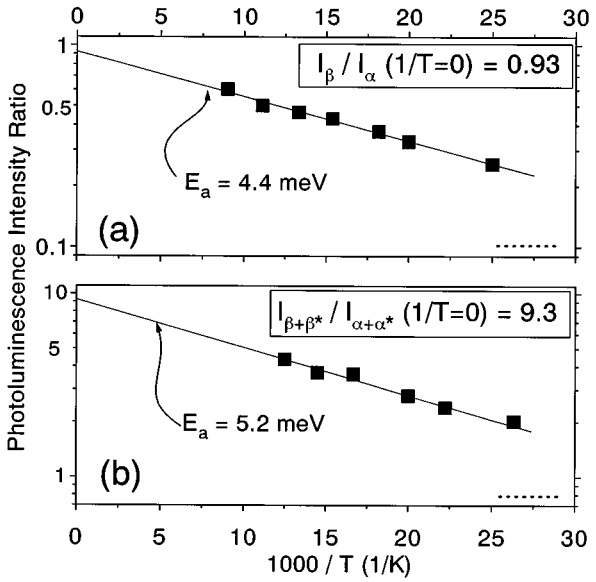

FIG. 4. Temperature dependence of the intensity ratios of PL lines β and α (QW2) in (a) and of the lines ($\beta+\beta^*$) and ($\alpha+\alpha^*$) (QW3) in (b). The intensity values are obtained from fits to the data points assuming two and four Gaussian shaped lines in (a) and (b), respectively. The solid lines describe the relationship between the exponential temperature dependence and the respective activation energies E_a. The low-temperature limits (5 K) are marked by dotted lines at the right margin.

energy as on B] before radiative recombination takes place. The transfer from A to B, however, is suppressed. Hence at low T the ratio I_β/I_α does not agree with the ratio of the corresponding density of states.[11] When T is raised, the intensity of line β increases at the expense of the intensity of line α. The Arrhenius plots of I_β/I_α from QW2 and $I_{\beta+\beta^*}/I_{\alpha+\alpha^*}$ from QW3 are drawn in Figs. 4(a) and 4(b), respectively. The logarithm of the intensity ratios shows a linear decrease with $1/T$ for the displayed temperature range, i.e.,

$$I_\beta/I_\alpha \propto S_B/S_{A^*}\exp(-E_a/kT),$$

where S_B/S_A reflects the ratio of the density of states of the corresponding QW regions, E_a is the thermal activation energy, and k is Boltzmann's constant. The slope of the straight lines in Figs. 4(a) and 4(b) corresponds to values of E_a of 4.4 and 5.2 meV, respectively. This is consistent with the fact that these activation energies should be smaller than $\Delta E_{1\ \mathrm{ML}}$. Extrapolating these straight lines to infinite T, S_B/S_A is estimated to be about 1 for QW2 and 10 for QW3. In this estimate we have neglected the proportionality factor, because the absorption strengths of regions A and B are expected to be nearly the same. Hence in Fig. 1(b) the PLE signal at the position of α should be as large as that at the position of β, but it is actually only $\frac{1}{10}$ of the expected value. In the case of QW3 [Fig. 1(c)] the PLE signal is almost zero at the position of α, where we could expect about $\frac{1}{10}$ of the PLE signal measured for β.

The strong suppression of the PLE signal can be understood in terms of exciton localization at interface defects as discussed above. Excitons, which are excited resonantly at the almost defect-free regions of terraces B during the wavelength scan of the PLE measurement, are only localized weakly. Therefore some of them are able to move to QW regions A and have sufficient excess energy to find the very deep minima A_{det} representing the detection energy E_{det} of the PLE. Thus they contribute to the PLE signal. However, excitons, which are resonantly excited within QW regions A, are in general strongly localized[22,33] and not able to move to other QW regions, especially to regions A_{det}. Hence the intensity of the PLE signal is suppressed and does not necessarily correspond to the absorption strength in this spectral range. Note that in the low-temperature case of Fig. 1 the PLE signal is strongly suppressed only in energy regions showing clear spikes in the micro-PL spectrum. This suppression is less pronounced at higher temperatures, and PLE is expected to be a measure for the optical density of states (absorption). The fact that we find an Arrhenius behavior above $\approx$40 K (cf. Fig. 4) indicates that such ''kinetic'' suppression of PLE is no longer effective at this temperature.

IV. SUMMARY AND CONCLUSIONS

In conclusion, we compared PL, micro-PL, and PLE spectra of thin GaAs/$Al_xGa_{1-x}As$ single QWs fabricated under different conditions by growth-interrupted MBE. At low temperatures excitons are localized at interface defects of different lateral sizes. Therefore the PL spectrum consists actually of a certain distribution of very narrow lines. This distribution is related to an interface roughness on a length scale smaller than the exciton Bohr radius. Its average energy shift with respect to the PLE spectrum is a measure for the average defect size. Moreover, the splitting of the PL spectrum into two main lines indicates an additional variation of the mean QW thickness on a length scale larger than R_B. The low- and high-energy PL lines include the strongly and weakly localized excitons, respectively. In this sense, the two different splittings of PL spectra (fine structure $\leqslant$0.1–0.2 meV, ML splitting $\leqslant$1–10 meV) reflect two components of the interface roughness, which differ in their lateral length scale. Therefore it should be possible to extract detailed information about the real interface structure, when exciton localization at interface defects is effective. An additional consequence of this kind of exciton localization is the strong suppression of the PLE signal within the low-energy part of the PL spectrum, which is therefore not necessarily a measure for the absorption strength or an indication for impurity-related PL of QWs.

ACKNOWLEDGMENTS

We would like to thank J. Menniger, R. Zimmermann, and F. Groβe for helpful discussions. Part of this work was performed within the framework of the Sfb 296 of the Deutsche Forschungsgemeinschaft.

*On leave at Research Center for Quantum Effect Electronics, Tokyo Institute of Technology, 2-12-1 O-okayama, Meguro-ku, Tokyo 152, Japan.

[1] C. A. Warwick, W. Y. Jan, A. Ourmazd, and T. D. Harris, Appl. Phys. Lett. **56**, 2666 (1990).

[2] D. Gammon, B. V. Shanabrook, and D. S. Katzer, Phys. Rev. Lett. **67**, 1547 (1991).

[3] Colin A. Warwick and Rose F. Kopf, Appl. Phys. Lett. **60**, 386 (1992).

[4] J. Menniger, H. Kostial, U. Jahn, R. Hey, and H. T. Grahn, Appl. Phys. Lett. **66**, 2349 (1995).

[5] D. Gammon, B. V. Shanabrook, and D. S. Katzer, Appl. Phys. Lett. **57**, 2710 (1990).

[6] M. A. Herman, D. Bimberg, and J. Christen, J. Appl. Phys. **70**, R1 (1991).

[7] E. Runge, J. Menniger, U. Jahn, R. Hey, and H. T. Grahn, Phys. Rev. B **52**, 12 207 (1995).

[8] S. K. Sinha, E. B. Sirota, S. Garoff, and H. B. Stanley, Phys. Rev. B **38**, 2297 (1988); B. Jenichen, S. A. Stepanov, B. Brar, and H. Kroemer, J. Appl. Phys. **79**, 120 (1996).

[9] J. Christen and D. Bimberg, Phys. Rev. B **42**, 7213 (1990).

[10] A. Ourmazd, D. W. Taylor, J. Cunningham, and C. W. Tu, Phys. Rev. Lett. **62**, 933 (1989).

[11] X. Liu, S. Nilsson, L. Samuelson, W. Seifert, and P. L. Sonza, Phys. Rev. B **47**, 2203 (1993).

[12] E. Runge, A. Schülzgen, F. Henneberger, and R. Zimmermann, Phys. Status Solidi B **188**, 547 (1995).

[13] R. Zimmermann and E. Runge, J. Lumin. **60&61**, 320 (1994).

[14] K. Brunner, G. Abstreiter, G. Böhm, G. Tränkle, and G. Weimann, Appl. Phys. Lett. **64**, 3320 (1994).

[15] H. F. Hess, E. Betzig, T. D. Harris, L. N. Pfeiffer, and K. W. West, Science **264**, 1740 (1994).

[16] Masaaki Tanaka and Hiroyuki Sakaki, J. Appl. Phys. **64**, 4503 (1988).

[17] E. S. Koteles, B. S. Elman, C. Jagannath, and Y. J. Chen, Appl. Phys. Lett. **49**, 1465 (1986).

[18] Ch. Maierhofer, S. Munnix, D. Bimberg, R. K. Bauer, D. E. Mars, and J. N. Miller, Appl. Phys. Lett. **55**, 50 (1989).

[19] K. Fujiwara, R. Cingolani, and K. Ploog, J. Phys. (France) IV **3**, C5-307 (1993).

[20] R. F. Kopf, E. F. Schubert, T. D. Harris, R. S. Becker, and G. H. Gilmer, J. Appl. Phys. **74**, 6139 (1993).

[21] R. F. Kopf, E. F. Schubert, T. D. Harris, and R. S. Becker, Appl. Phys. Lett. **58**, 631 (1991).

[22] D. C. Reynolds, K. R. Evans, C. E. Stutz, and P. W. Yu, Appl. Phys. Lett. **60**, 962 (1992).

[23] D. C. Reynolds, K. K. Bajaj, C. W. Litton, J. Singh, P. W. Yu, P. Pearah, J. Klem, and H. Morkoç, Phys. Rev. B **33**, 5931 (1986).

[24] D. Gammon, E. S. Snow, and D. S. Katzer, Appl. Phys. Lett. **67**, 2391 (1995).

[25] As has been observed for another QW series (not shown in this work), the spectral shift of the PL line relative to the PLE line varies also when growth parameters other than the misorientation angle, e.g., the substrate temperature, are changed. For all investigated samples the PLE signal is strongly suppressed in that spectral region where the micro-PL spectrum shows a pronounced fine structure.

[26] If the broad background in the micro-PL is attributed to small unresolved lines, an even higher estimate results.

[27] G. Bastard, C. Delalande, M. H. Meynadier, P. M. Frijlink, and M. Voos, Phys. Rev. B **29**, 7042 (1984).

[28] See, e.g., F. Groβe and R. Zimmermann, Superlatt. Microstruct. **17**, 439 (1995), and references therein.

[29] R. Zimmermann, Phys. Status Solidi B **173**, 129 (1992).

[30] R. Klann, H. T. Grahn, and K. Fujiwara, Phys. Rev. B **51**, 10 232 (1995).

[31] M. Gurioli, A. Vinattieri, J. Martinez-Pastor, and Marcello Colocci, Phys. Rev. B **50**, 11 817 (1994).

[32] F. Yang, M. Wilkinson, E. J. Austin, and K. P. O'Donnell, Phys. Rev. Lett. **70**, 323 (1993).

[33] M. Kohl, D. Heitmann, S. Tarucha, K. Leo, and K. Ploog, Phys. Rev. B **39**, 7736 (1989).